frontiers in Energy Research

BRIEF RESEARCH REPORT
published: 22 April 2020
doi: 10.3389/fenrg.2020.00060

# Rh-Decorated Three-Dimensional Graphene Aerogel Networks as Highly-Efficient Electrocatalysts for Direct Methanol Fuel Cells

*Ying Yang†, Yuexin Song†, Hao Sun, Danyang Xiang, Quanguo Jiang, Zhiyong Lu, Haiyan He and Huajie Huang**

*College of Mechanics and Materials, Hohai University, Nanjing, China*

The exploration and development of highly-efficient Pt-alternative catalysts with acceptable costs are very essential for the large-scale commercial applications of direct methanol fuel cell (DMFC) technology. Herein, we demonstrate a facile and cost-effective self-assembly approach to the bottom-up fabrication of Rh-decorated three-dimensional graphene aerogel (Rh/3D-GA) networks as efficient DMFC anode catalysts. With the distinct textural features including large surface area, 3D porous structure, uniform Rh dispersion, and good electron conductivity, the resultant Rh/3D-GA hybrid architecture shows superior electrocatalytic properties toward methanol oxidation reaction, such as large electrochemically active surface area, low onset potential, high mass activity as well as excellent long-term stability, all of which are more competitive than those of Rh catalysts deposited on conventional carbon black, carbon nanotubes, and two-dimensional graphene supports.

**Keywords: Rhodium, graphene aerogel, three-dimensional networks, electrocatalyst, fuel cells**

OPEN ACCESS

***Edited by:***
*Kaiyuan Shi,*
*National Research Council Canada, Canada*

***Reviewed by:***
*Xifei Li,*
*Xi'an University of Technology, China*
*Babak Shalchi Amirkhiz,*
*Department of Natural Resources, Canada*

***Correspondence:**
*Huajie Huang*
*huanghuajie@hhu.edu.cn*

*†These authors have contributed equally to this work*

***Specialty section:***
*This article was submitted to Electrochemical Energy Conversion and Storage, a section of the journal Frontiers in Energy Research*

***Received:*** *14 February 2020*
***Accepted:*** *30 March 2020*
***Published:*** *22 April 2020*

***Citation:***
*Yang Y, Song Y, Sun H, Xiang D, Jiang Q, Lu Z, He H and Huang H (2020) Rh-Decorated Three-Dimensional Graphene Aerogel Networks as Highly-Efficient Electrocatalysts for Direct Methanol Fuel Cells. Front. Energy Res. 8:60. doi: 10.3389/fenrg.2020.00060*

## INTRODUCTION

Since the problem of energy crisis and environment pollution is becoming more and more severe, fuel cells have attracted considerable attention as advanced energy-conversion systems because of their high energy-utilization efficiency and low pollutant emission properties (Chu and Majumdar, 2012). Among different types of fuel cells, direct methanol fuel cells (DMFCs) have many distinct advantages, such as simple device construction, low working temperature, and convenient storage and transport of methanol, which have been regarded as ideal power generators for a variety of applications, including aeronautics and astronautics, electric vehicles as well as portable electronic devices (Huang and Wang, 2014). Notably, the occurrence of methanol oxidation reaction with slow kinetic rate on the anode requires highly-active electrocatalysts, which largely determine the energy density and power density of the DMFC devices (Debe, 2012).

As is well-known, platinum (Pt) is the most popular electrode catalyst for DMFCs due to its unique electrocatalytic ability for methanol oxidation reaction (Huang et al., 2014; Yang et al., 2019). However, the scarcity and poor poison tolerance of Pt-based catalysts commonly render high manufacturing costs and short lifespan of DMFCs, which remain the critical obstacles impeding their large-scale commercial applications (Chang et al., 2014; Huang et al., 2017a). Within this context, highly-active non-platinum electrocatalysts with acceptable costs have been widely studied by many researchers (Fu et al., 2018; Yang et al., 2020). Among various current Pt-alternative

materials, Rhodium (Rh) nanocrystals have recently become a hot topic of interest owing to their exceptional methanol oxidation activity as well as greater resistance to byproducts (mainly CO) in alkaline medium (Han et al., 2018; Kang et al., 2018; Li F. et al., 2018). Nevertheless, similar to other noble metals, the electrocatalytic properties of Rh nanocrystals are strongly dependent on their size and morphology, thereby the rational design and controllable synthesis of small-sized and well-dispersed Rh catalysts are highly desirable.

To achieve a high utilization efficiency of noble metal nanocrystals, one effective method is to deposit them onto various carbonaceous supports, such as carbon black (Zhang et al., 2015), carbon nanotubes (Zhang et al., 2018), porous carbons (Gao et al., 2018), and graphene (Shen et al., 2018; Huang et al., 2019). In particular, graphene-supported noble metal catalysts usually possess superior electrocatalytic performance toward methanol oxidation owing to their large surface area, high electron conductivity, and good electrochemical stability (Huang et al., 2016; Zhou et al., 2016). However, two-dimensional (2D) graphene-based materials are prone to re-aggregate or re-stack due to the van der Waals forces when they are extracted from solutions, a process during which the intrinsic physicochemical properties of the separated graphene layers would disappear (Yan et al., 2018). Meanwhile, a high proportion of catalytically active regions could be covered and cannot directly engage into the eletrocatalytic reaction, leading to a large loss of electrocatalytic activity (Li M. et al., 2018). To overcome this obstacle, great efforts have been made to the construction of three-dimensional (3D) graphene aerogel networks with cross-linked porous configuration, which can well-preserve the unique structural merits of separated graphene nanosheets and simultaneously promote the transportation of external electrolytes to the interior catalytic sites (Huang et al., 2015, 2017b; Zhang et al., 2016). However, up to now, the uniform growth of small-sized Rh nanocrystals onto 3D graphene aerogel networks still remains a challenge in this area.

Herein, we present a bottom-up approach to the large-scale fabrication of ultrafine Rh nanoparticles supported on 3D interconnected graphene aerogel networks as methanol oxidation catalysts via a solvothermal self-assembly process. As illustrated in **Supplementary Figure 1**, graphene oxide (GO) nanosheets were first produced from commercial graphite powders via an improved Hummers' method and then ultrasonically dispersed in ethylene glycol solution to reach a concentration of 2 mg $mL^{-1}$. Next, $Rh(NO_3)_3$ solution was slowly added into above GO suspension under magnetic stirring for 30 min. Subsequently, the resultant mixture was moved to a Teflon-lined stainless steel autoclave and kept at 160°C for 24 h. During the solvothermal reaction, the adjacent GO nanosheets with numerous oxygen functional groups were able to interconnect with each other, and at the same time Rh nanoparticles were gradually deposited on the carbon sheets, giving birth to the Rh/3D graphene aerogel (Rh/3D-GA) architecture. Benefiting from its large surface area, 3D porous frameworks, and homogeneous Rh dispersion, the resulting Rh/3D-GA architecture exhibits superior electrocatalytic properties toward methanol oxidation, including large electrochemically active surface area, high mass activity, and reliable long-term stability, all of which are more competitive than those of Rh/carbon black (Rh/C), Rh/CNT, and Rh/reduced graphene oxide (Rh/RGO) catalysts.

# EXPERIMENTAL

## Preparation of the Rh/3D-GA Architecture

First, GO nanosheets as starting materials were produced from natural graphite powders through an improved Hummers' method (Kovtyukhova et al., 1999). Then, 40 mg of GO nanosheets were dispersed in 10 mL water and 10 mL of ethylene glycol to form a stable dark brown solution with the help of ultrasonic treatment for 1 h. Afterwards, 0.076 mL of $Rh(NO_3)_3$ solution (1.28 M) was introduced into above GO solution under magnetic stirring for 30 min. Next, the resultant mixture was moved to a Teflon-lined stainless steel autoclave and heated at 160°C for 24 h. The as-derived product was dialyzed with pure water for 3 days and then freeze-dried to preserve its 3D porous networks, leading to the formation of the Rh/3D-GA architecture. As for the preparation of Rh particles supported by conventional carbon black (Vulcan XC-72R, Cabot Corp.), multiwalled CNTs (Chengdu Organic Chemicals Co., Ltd.), and RGO materials, 20 mg of carbon materials were dispersed in 40 mL water and 40 mL of ethylene glycol solution, and then the deposition of Rh nanoparticles on these carbon supports was realized by the similar synthesis approach. For fair comparison, the Rh contents of all above catalysts were kept at 20.0 wt%.

## Characterization

The 3D porous structure and Rh dispersion of the Rh/3D-GA architecture were observed by Field-emission scanning microscopy (FE-SEM, Hitachi S-4800) and transmission electron microscopy (TEM, JEOL 2100F). The crystal structures of various samples were analyzed by Powder X-ray diffraction (XRD, Bruker D8 Advance diffractometer). The elemental composition and chemical states of Rh/3D-GA were examined by X-ray photoelectron spectroscopy (XPS, PHI Quantera X-ray photoelectron spectrometer). Nitrogen adsorption–desorption tests were conducted on a Micromeritics ASAP 2020 Plus system at 77 K.

## Electrochemical Measurements

All electrochemical measurements were conducted on a CHI 760E electrochemical workstation by using a standard three-electrode configuration, where a 3 mm glassy carbon (GC) disk with active electrocatalyst, a Pt wire, and a saturated calomel electrode (SCE) were served as the working, counter, and reference electrodes, respectively. The fabrication procedure for the working electrode is as follows: 5 mg of catalyst powder was dispersed into a mixed solution (2,375 μL of ethanol, 2,375 μL of water, and 250 μL of 5% Nafion) via ultrasonic treatment for 1 h. Subsequently, 10 μL of above catalyst dispersion was carefully pipetted onto a GC electrode surface and then directly dried in air. Therefore, the Rh loading amount on

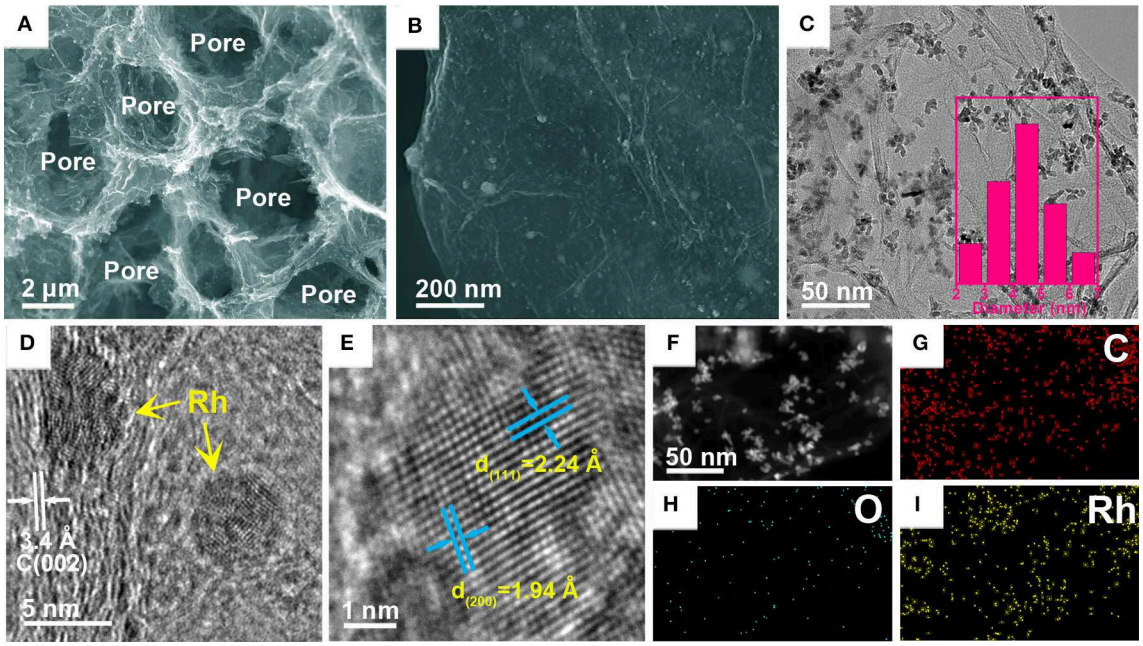


**FIGURE 1 |** Representative **(A,B)** FE-SEM, **(C)** TEM, and **(D,E)** HRTEM images of the Rh/3D-GA architecture. The inset in **(C)** is the Rh size distribution. **(F)** HAADF–STEM image and the corresponding elemental mapping analysis of **(G)** C, **(H)** O, and **(I)** Rh elements of a Rh-decorated graphene nanosheet.

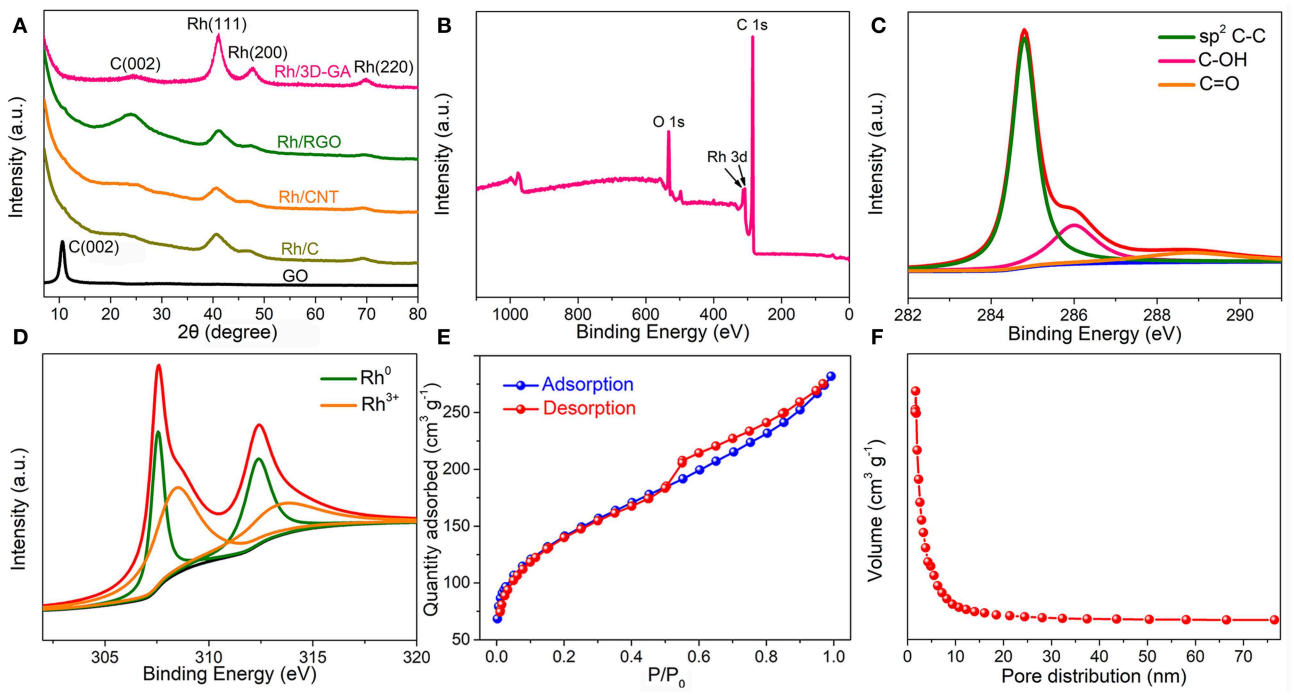


**FIGURE 2 | (A)** Typical XRD patterns of the Rh/3D-GA, Rh/RGO, Rh/CNT, Rh/C, and GO materials. **(B)** XPS survey, **(C)** C 1s, and **(D)** Rh 3d spectra of the Rh/3D-GA architecture. **(E)** Nitrogen adsorption–desorption isotherm and **(F)** pore size distribution of the Rh/3D-GA architecture.

the working electrode surface was kept at 0.028 mg $cm^{-2}$. The electrocatalytic properties of the Rh/3D-GA architecture and other reference catalysts were systematically investigated by cyclic voltammograms, chronoamperometry, and AC impedance techniques.

## RESULTS AND DISCUSSION

The 3D porous structure and morphology of the as-obtained Rh/3D-GA architecture were first observed by FE-SEM and TEM. As shown in **Figure 1A**, typical FE-SEM image

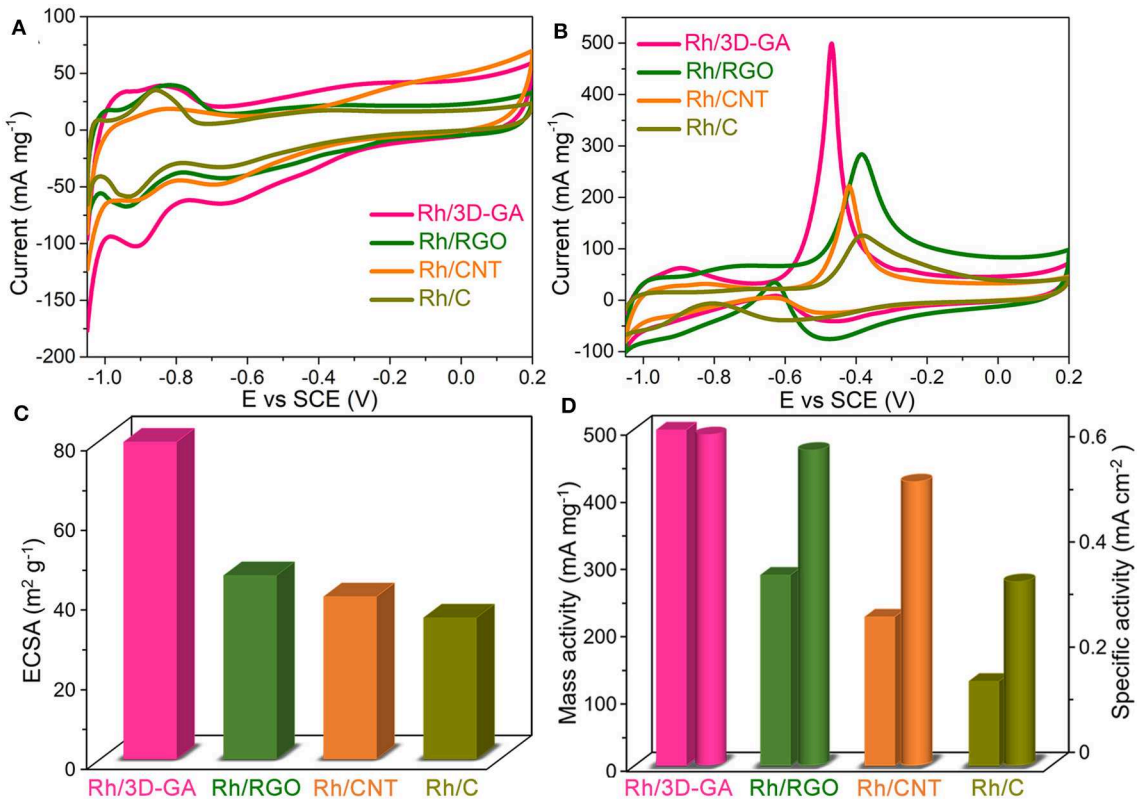


**FIGURE 3 |** CV curves of the Rh/3D-GA, Rh/RGO, Rh/CNT, and Rh/C electrodes recorded in **(A)** 1 M KOH and **(B)** 1 M KOH with 1 M $CH_3OH$ solution at 50 mV $s^{-1}$. **(C)** Specific ECSA values and **(D)** mass activity as well as specific activity (normalized by ECSA) for these four catalysts.

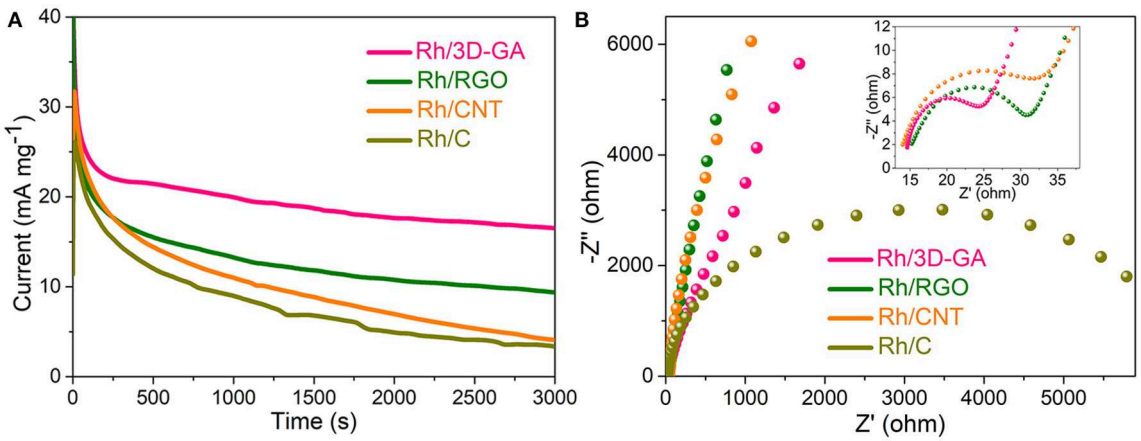


**FIGURE 4 | (A)** Chronoamperometric curves of the Rh/3D-GA, Rh/RGO, Rh/CNT, and Rh/C electrodes recorded in 1 M KOH with 1 M $CH_3OH$ solution at −0.5 V. **(B)** AC impedance spectra of the above four catalysts in 1 M KOH with 1 M $CH_3OH$ solution tested at open circuit potentials with an amplitude of 10 mV.

discloses that Rh/3D-GA possesses well-defined 3D cross-linked networks with consecutive macropores ranging from hundreds of nanometers to several micrometers. Such a 3D porous configuration can not only hamper the re-aggregation and re-stacking of graphene nanosheets, but also provides multilevel growth platforms for the deposition of Rh nanoparticles. Clearly, high-magnification FE-SEM and TEM images confirm that the ultrathin graphene sheets are decorated uniformly with a large number of Rh nanoparticles with an average diameter of about 4.3 nm (**Figures 1B,C**), which is close to that of previously reported Pt and Pd particles supported by nanocarbon matrixes (Li et al., 2012; Qian et al., 2015). Moreover,

with the help of high-resolution TEM (**Figures 1D,E**), typical lattice fringes with crystal plane distance of 0.34 nm can be observed, which corresponds to the carbon (002) plane of few-layer graphene nanosheets. Meanwhile, the interplane spacings on Rh nanoparticles were determined to be 0.22 and 0.19 nm, consistent with the data for the (111) and (200) planes of cubic Rh crystals, respectively. Furthermore, high-angle annular dark-field-scanning TEM (HAADF-STEM) and element mapping analysis reveal that the Rh/3D-GA architecture consists of C, Rh, and a smaller amount of O components (**Figures 1F–I** and **Supplementary Figure 2**), which are distributed homogeneously throughout the whole sheets.

Powder XRD and XPS analysis were then carried out to study the detailed crystalline structure and elemental composition of the Rh/3D-GA architecture. As depicted in **Figure 2A**, the prominent C (002) diffraction peak of pristine GO centered at $2\theta = 10.5^{\circ}$ shifted to a much higher angle of $2\theta = 25.5^{\circ}$ in the Rh/3D-GA and Rh/RGO patterns, implying the successful transformation of GO to graphene. In addition, other four diffraction peaks located at $2\theta = 41.0^{\circ}$, $47.8^{\circ}$, $69.9^{\circ}$, and $84.1^{\circ}$ are also visible, which can be indexed to the (111), (200), (220), and (311) planes of the face centered-cubic (fcc) Rh nanocrystals. Remarkably, the above four peaks in the Rh/3D-GA pattern are more intensive than those in the Rh/RGO, Rh/CNT, and Rh/C patterns, indicating that the use of 3D graphene aerogel networks as supporting materials can promote the nucleation and crystallization of Rh nanoparticles. **Figure 2B** shows the typical XPS survey spectrum of Rh/3D-GA catalyst, where the C 1s, O 1s, and Rh 3d signals were detected, consistent with the EDX results (**Supplementary Figure 3**). Moreover, the high-resolution C 1s XPS spectrum unravels that there are three kinds of C species in the Rh/3D-GA catalyst, including $sp^2$ C–C, C-OH, and C=O groups at the binding energies of 284.8, 286.1, and 288.4 eV, respectively (**Figure 2C**). Apparently, the peak intensities for the C-OH and C=O groups in Rh/3D-GA spectrum are much lower than those in GO spectrum (**Supplementary Figure 4**), proving again the efficient reduction of GO during the solvothermal process. Besides, the deconvoluted Rh 3d spectrum in **Figure 2D** suggests two chemical states of Rh in the sample: the two intensive peaks at 307.5 and 312.4 eV are related to metal Rh, while the two weak peaks at 308.4 and 313.4 eV belong to Rh oxide. Brunauer–Emmett–Teller (BET) analysis further demonstrates that the Rh/3D-GA architecture with meso- and macroporous features has a high BET surface area of 485.0 $m^2\ g^{-1}$ (**Figures 2E,F**), in accord with that reported for 3D graphene nanomaterials (Huang and Wang, 2014).

Inspired by the 3D porous graphene structure as well as the well-dispersive Rh nanocrystals, a series of electrochemical measurements were performed to systematically investigate the electrocatalytic properties of Rh/3D-GA architecture toward methanol oxidation reaction in alkaline medium, together with those of the Rh/RGO, Rh/CNT, and Rh/C catalysts for comparison. **Figure 3A** presents the cyclic voltammetry (CV) curves of the four electrodes recorded in 1 M KOH solution. It can be seen that all these CV curves exhibit characteristic hydrogen adsorption/desorption peaks in the potential region from −0.75 to −1.05 V (vs. SCE), which can be employed to evaluate the electrochemical active surface areas (ECSAs) for Rh-based catalysts. As calculated, the ECSA value for the Rh/3D-GA electrode is found to be 79.6 $m^2\ g^{-1}$, which is about 1.7, 2.0, and 2.2 times larger than that of Rh/RGO (46.1 $m^2\ g^{-1}$), Rh/CNT (40.8 $m^2\ g^{-1}$), and Rh/C (35.5 $m^2\ g^{-1}$) electrodes, respectively, indicating that the existence of 3D interconnected networks in Rh/3D-GA catalyst is very favorable for the exposure of catalytically active Rh sites. In the presence of 1 M KOH and 1 M $CH_3OH$ solution, the intensive current peaks appeared in the forward scans of the CV curves arise from the methanol oxidation, while the relatively weak current peaks in the reverse scan is due to the oxidative removal of the absorbed CO species (**Figure 3B**). Clearly, a very high forward peak current density (498.9 mA $mg^{-1}$) and high ECSA-normalized specific activity (0.63 mA $cm^{-2}$) are achieved on the Rh/3D-GA electrode (**Figures 3C,D**), which are higher than those on the reference electrodes (125.7–283.4 mA $mg^{-1}$ and 0.35–0.59 mA $cm^{-2}$, respectively). Furthermore, both the ECSA and mass activity of our Rh/3D-GA catalyst are superior to those of commercial 20% Pt/C catalyst (**Supplementary Figure 5**) and recent state-of-the-art Rh-based nanostructures, such as Rh nanosheets/graphene (Kang et al., 2017), Rh nanodendrites (Kang et al., 2016), and PtRh alloy (Bai et al., 2018), demonstrating that Rh/3D-GA is a highly promising anode catalyst for DMFCs.

Long-term durability of an electrocatalyst is another key performance indicator for its industrial applications. In this aspect, chronoamperometric technique was used to assess the long-term stability of Rh catalysts supported by different supports (**Figure 4A**). With a constant electrode potential, it can be clearly seen that the methanol oxidation currents on all electrodes gradually decrease as the time goes on, which should be ascribed to the accumulation of CO poisoning species on the Rh sites as well as the generation of Rh agglomerations in the architecture system. Among these investigated electrodes, the Rh/3D-GA electrode showed the slowest current decay rate and maintained the highest activity over 3,000 s, giving the best catalytic stability for methanol electrooxidation. The significantly improved durability of Rh/3D-GA catalyst should be attributed to the strong interaction between Rh and 3D-GA networks, which could prevent the Rh particles from agglomeration, dissolution, or Ostwald ripening during the catalytic process.

In order to gain more insights into the electron conductivity of various catalysts, we further conducted the AC impedance measurements to compare the charge-transfer rates. As shown in **Figure 4B**, the Nyquist plots of all these electrodes possess a depressed semiarc in the high frequency range, which is commonly employed to evaluate the catalyst's charge-transfer resistance. Based on the equivalent circuit displayed in **Supplementary Figure 6**, the charge-transfer resistance of Rh/3D-GA catalyst was estimated to be only 9.1 $\Omega$, much lower than that of Rh/RGO (18.0 $\Omega$), Rh/CNT (20.1 $\Omega$), and Rh/C (6519.0 $\Omega$) catalysts, testifying that the 3D cross-linked graphene networks could serve as efficient pathways for charge

transportation. The excellent electronic conductivity of Rh/3D-GA is able to offer a large population of the triple-phase boundaries in the catalytic system, which is very conducive to boosting the electrochemical kinetics for methanol oxidation reaction.

## CONCLUSION

In summary, the bottom-up construction of Rh-decorated 3D graphene aerogel networks has been achieved through a solvothermal self-assembly approach. The resulting hybrid architecture has a series of structural advantages, such as large surface area, 3D interconnected carbon skeletons, uniform Rh dispersion, and high electron conductivity, which can not only provide a large number of catalytically active sites, but also allow a rapid transportation of ions and electrons during the electrocatalytic process. As a consequence, the Rh/3D-GA architecture shows large electrochemically active surface area, high mass activity as well as good long-term durability toward methanol oxidation reaction, superior to those of the Rh/RGO, Rh/CNT, and Rh/C catalysts synthesized by the same method. This study could provide new insights into the controllable synthesis of Pt-alternative catalysts supported by 3D porous carbon materials and facilitate their commercial applications in the electrocatalytic fields.

## DATA AVAILABILITY STATEMENT

The datasets generated for this study are available on request to the corresponding author.

## AUTHOR CONTRIBUTIONS

HHu conceived and designed the experiments. YY and YS conducted the experiments. HS, DX, QJ, ZL, and HHe recorded the structural characterization data. YY and HHu wrote the manuscript.

## FUNDING

This work was financially supported by the National Natural Science Foundation of China (51802077), the Fundamental Research Funds for the Central Universities (2019B16214), China Postdoctoral Science Foundation (Nos. 2015M580387 and 2016T90414), and Jiangsu Planned Projects for Postdoctoral Research Funds (No. 1601026A).

## SUPPLEMENTARY MATERIAL

The Supplementary Material for this article can be found online at: https://www.frontiersin.org/articles/10.3389/fenrg.2020.00060/full#supplementary-material

## REFERENCES

Bai, J., Xiao, X., Xue, Y. Y., Jiang, J. X., Zeng, J. H., Li, X. F., et al. (2018). Bimetallic Platinum-Rhodium alloy nanodendrites as highly active electrocatalyst for the ethanol oxidation reaction. *ACS Appl. Mater. Interfaces* 10, 19755–19763. doi: 10.1021/acsami.8b05422

Chang, J., Feng, L., Liu, C., Xing, W., and Hu, X. (2014). $Ni_2P$ enhances the activity and durability of the Pt anode catalyst in direct methanol fuel cells. *Energy Environ. Sci.* 7, 1628–1632. doi: 10.1039/c4ee00100a

Chu, S., and Majumdar, A. (2012). Opportunities and challenges for a sustainable energy future. *Nature* 488, 294–303. doi: 10.1038/nature11475

Debe, M. K. (2012). Electrocatalyst approaches and challenges for automotive fuel cells. *Nature* 486, 43–51. doi: 10.1038/nature11115

Fu, X., Zhao, Z., Wan, C., Wang, Y., Fan, Z., Song, F., et al. (2018). Ultrathin wavy Rh nanowires as highly effective electrocatalysts for methanol oxidation reaction with ultrahigh ECSA. *Nano Res.* 12, 211–215. doi: 10.1007/s12274-018-2204-8

Gao, Z., Li, M., Wang, J., Zhu, J., Zhao, X., Huang, H., et al. (2018). Pt nanocrystals grown on three-dimensional architectures made from graphene and $MoS_2$ nanosheets: highly efficient multifunctional electrocatalysts toward hydrogen evolution and methanol oxidation reactions. *Carbon* 139, 369–377. doi: 10.1016/j.carbon.2018.07.006

Han, S.-H., Liu, H.-M., Chen, P., Jiang, J.-X., and Chen, Y. (2018). Porous trimetallic PtRhCu cubic nanoboxes for ethanol electrooxidation. *Adv. Energy. Mater.* 8:1801326. doi: 10.1002/aenm.201801326

Huang, H., Ma, L., Tiwary, C. S., Jiang, Q., Yin, K., Zhou, W., et al. (2017a). Worm-shape Pt nanocrystals grown on nitrogen-doped low-defect graphene sheets: highly efficient electrocatalysts for methanol oxidation reaction. *Small.* 13:1603013. doi: 10.1002/smll.201603013

Huang, H., and Wang, X. (2014). Recent progress on carbon-based support materials for electrocatalysts of direct methanol fuel cells. *J. Mater. Chem. A.* 2, 6266–6291. doi: 10.1039/C3TA14754A

Huang, H., Yan, M., Yang, C., He, H., Jiang, Q., Yang, L., et al. (2019). Graphene nanoarchitectonics: recent advances in graphene-based electrocatalysts for hydrogen evolution reaction. *Adv. Mater.* 31:1903415. doi: 10.1002/adma.201903415

Huang, H., Yang, S., Vajtai, R., Wang, X., and Ajayan, P. M. (2014). Pt-decorated 3D architectures built from graphene and graphitic carbon nitride nanosheets as efficient methanol oxidation catalysts. *Adv. Mater.* 26, 5160–5165. doi: 10.1002/adma.201401877

Huang, H., Ye, G., Yang, S., Fei, H., Tiwary, C. S., Gong, Y., et al. (2015). Nanosized Pt anchored onto 3D nitrogen-doped graphene nanoribbons towards efficient methanol electrooxidation. *J. Mater. Chem. A* 3, 19696–19701. doi: 10.1039/C5TA05372B

Huang, H., Zhu, J., Li, D., Shen, C., Li, M., Zhang, X., et al. (2017b). Pt nanoparticles grown on 3D $RuO_2$-modified graphene architectures for highly efficient methanol oxidation. *J. Mater. Chem. A* 5, 4560–4567. doi: 10.1039/c6ta10548c

Huang, H., Zhu, J., Zhang, W., Tiwary, C. S., Zhang, J., Zhang, X., et al. (2016). Controllable codoping of nitrogen and sulfur in graphene for highly efficient Li-oxygen batteries and direct methanol fuel cells. *Chem. Mater.* 28, 1737–1745. doi: 10.1021/acs.chemmater.5b04654

Kang, Y., Li, F., Li, S., Ji, P., Zeng, J., Jiang, J., et al. (2016). Unexpected catalytic activity of rhodium nanodendrites with nanosheet subunits for methanol electrooxidation in an alkaline medium. *Nano Res.* 9, 3893–3902. doi: 10.1007/s12274-016-1258-8

Kang, Y., Xue, Q., Jin, P., Jiang, J., Zeng, J., and Chen, Y. (2017). Rhodium nanosheets–reduced graphene oxide hybrids: a highly active platinum-alternative electrocatalyst for the methanol oxidation reaction in alkaline media. *ACS Sustainable Chem. Eng.* 5, 10156–10162. doi: 10.1021/acssuschemeng.7b02163

Kang, Y. Q., Xue, Q., Zhao, Y., Li, X. F., Jin, P. J., and Chen, Y. (2018). Selective etching induced synthesis of hollow Rh nanospheres electrocatalyst for alcohol oxidation reactions. *Small* 14:1801239. doi: 10.1002/smll.201801239

Kovtyukhova, N. I., Ollivier, P. J., Martin, B. R., Mallouk, T. E., Chizhik, S. A., Buzaneva, E. V., et al. (1999). Layer-by-layer assembly of ultrathin composite

films from micron-sized graphite oxide sheets and polycations. *Chem. Mater.* 11, 771–778. doi: 10.1021/Cm981085u

Li, F., Ding, Y., Xiao, X., Yin, S., Hu, M., Li, S., et al. (2018). From monometallic Au nanowires to trimetallic AuPtRh nanowires: interface control for the formic acid electrooxidation. *J. Mater. Chem. A* 6, 17164–17170. doi: 10.1039/c8ta05710a

Li, M., Jiang, Q., Yan, M., Wei, Y., Zong, J., Zhang, J., et al. (2018). Three-dimensional boron- and nitrogen-codoped graphene aerogel-supported Pt nanoparticles as highly active electrocatalysts for methanol oxidation reaction. *ACS Sustainable Chem. Eng.* 6, 6644–6653. doi: 10.1021/acssuschemeng.8b00425

Li, Y., Li, Y., Zhu, E., McLouth, T., Chiu, C. Y., Huang, X., et al. (2012). Stabilization of high-performance oxygen reduction reaction Pt electrocatalyst supported on reduced graphene oxide/carbon black composite. *J. Am. Chem. Soc.* 134, 12326–12329. doi: 10.1021/ja3031449

Qian, H., Huang, H., and Wang, X. (2015). Design and synthesis of palladium/graphitic carbon nitride/carbon black hybrids as high-performance catalysts for formic acid and methanol electrooxidation. *J. Power Sources* 275, 734–741. doi: 10.1016/j.jpowsour.2014.10.109

Shen, W., Ge, L., Sun, Y., Liao, F., Xu, L., Dang, Q., et al. (2018). Rhodium nanoparticles/F-doped graphene composites as multifunctional electrocatalyst superior to Pt/C for hydrogen evolution and formic acid oxidation reaction. *ACS Appl. Mater. Interfaces* 10, 33153–33161. doi: 10.1021/acsami.8b09297

Yan, M., Jiang, Q., Zhang, T., Wang, J., Yang, L., Lu, Z., et al. (2018). Three-dimensional low-defect carbon nanotube/nitrogen-doped graphene hybrid aerogel-supported Pt nanoparticles as efficient electrocatalysts toward the methanol oxidation reaction. *J. Mater. Chem. A* 6, 18165–18172. doi: 10.1039/C8TA05124K

Yang, C., Jiang, Q., Li, W., He, H., Yang, L., Lu, Z., et al. (2019). Ultrafine Pt nanoparticle-decorated 3D hybrid architectures built from reduced graphene oxide and MXene nanosheets for methanol oxidation. *Chem. Mater.* 31, 9277–9287. doi: 10.1021/acs.chemmater.9b02115

Yang, Y., Huang, H., Shen, B., Jin, L., Jiang, Q., Yang, L., et al. (2020). Anchoring nanosized Pd on three-dimensional boron- and nitrogen-codoped graphene aerogels as a highly active multifunctional electrocatalyst for formic acid and methanol oxidation reactions. *Inorg. Chem. Front.* 7, 700–708. doi: 10.1039/c9qi01448a

Zhang, F., Zhou, D., Zhang, Z., Zhou, M., and Wang, Q. (2015). Preparation of Rh/C and its high electro-catalytic activity for ethanol oxidation in alkaline media. *RSC Adv.* 5, 91829–91835. doi: 10.1039/c5ra16859g

Zhang, L. Y., Zhao, Z. L., Yuan, W. Y., and Li, C. M. (2016). Facile one-pot surfactant-free synthesis of uniform $Pd_6Co$ nanocrystals on 3D graphene as an efficient electrocatalyst toward formic acid oxidation. *Nanoscale* 8, 1905–1909. doi: 10.1039/c5nr08512h

Zhang, W., Zhang, X., Chen, L., Dai, J., Ding, Y., Ji, L., et al. (2018). Single-walled carbon nanotube induced optimized electron polarization of rhodium nanocrystals to develop an interface catalyst for highly efficient electrocatalysis. *ACS Catal.* 8, 8092–8099. doi: 10.1021/acscatal.8b02016

Zhou, Y., Hu, X.-C., Fan, Q., and Wen, H.-R. (2016). Three-dimensional crumpled graphene as an electro-catalyst support for formic acid electro-oxidation. *J. Mater. Chem. A* 4, 4587–4591. doi: 10.1039/C5TA09956K

**Conflict of Interest:** The authors declare that the research was conducted in the absence of any commercial or financial relationships that could be construed as a potential conflict of interest.

*Copyright © 2020 Yang, Song, Sun, Xiang, Jiang, Lu, He and Huang. This is an open-access article distributed under the terms of the Creative Commons Attribution License (CC BY). The use, distribution or reproduction in other forums is permitted, provided the original author(s) and the copyright owner(s) are credited and that the original publication in this journal is cited, in accordance with accepted academic practice. No use, distribution or reproduction is permitted which does not comply with these terms.*